International Atomic Energy Agency

INDC(CCP)- 36/U

INDC INTERNATIONAL NUCLEAR DATA COMMITTEE

USSR State Committee on the Utilization

of Atomic Energy

NUCLEAR PHYSICS RESEARCH IN THE USSR

COLLECTED ABSTRACTS

ISSUE 16

Translated by the IAEA
October 1974

74-4492
Translated from Russian

INDC(CCP)-36/U

USSR State Committee on the Utilization
of Atomic Energy

NUCLEAR PHYSICS RESEARCH IN THE USSR
COLLECTED ABSTRACTS

ISSUE 16

Translated by the IAEA
October 1974

Institute of Physics and Power Engineering

PROGRAMME FOR CALCULATING REACTION CROSS-SECTIONS IN THE RESONANCE REGION

V.P. Lunev and A.A. Luk'yanov

The paper describes a programme of calculating the energy dependence of reaction cross-sections in the resonance energy region on the basis of the well-known parameters of the $\hat{S}$-matrix theory. The cross-sections are calculated with allowance for inter-resonance interference, Doppler broadening of resonances and experimental energy resolution.

The programme can be used to determine the fission cross-sections of ^{239}Pu, ^{235}U, etc., in which inter-resonance interference is strong.

CALCULATIONS OF FAST-NEUTRON RADIATIVE CAPTURE CROSS-SECTIONS BY THE STATISTICAL THEORY OF NUCLEAR REACTIONS

A.G. Dovbenko, A.V. Ignatyuk and V.A. Tolstikov

Fast-neutron radiative capture cross-sections have been calculated within the framework of the Hauser-Feshbach theory in many publications. Owing to the accumulation of substantial experimental material in recent times, it became necessary to carry out a more critical review of the results of such calculations. The authors study the influence of the different parameters on the behaviour of the capture cross-section. They consider the influence of fluctuations in neutron widths on the partial capture cross-sections and their relationship with the power functions derived from experimental data. An analysis is performed of different models for the level density and their influence on the energy dependence of radiation width.

CONTRIBUTION OF DIFFERENT REACTION MECHANISMS TO FAST-NEUTRON RADIATIVE CAPTURE CROSS-SECTIONS

A.G. Dovbenko and A.V. Ignatyuk

The process of radiative capture of fast neutrons by atomic nuclei is, at present, described theoretically on the basis of two limiting reaction mechanisms: the direct or semi-direct (collective) capture model and the compound nucleus model. Calculations have shown that the semi-direct capture model for heavy nuclei quite satisfactorily describes the hard part of the emitted gamma spectrum but gives too low a value for the cross-section in the range of medium neutron energies (< 10 MeV). The possibility of explaining the hard nature of the spectra on the basis of an improved compound-nucleus decay model has been investigated. Ordinarily, in calculating the average radiation widths of highly-excited nuclei, use is made of the evaporation approximation, according to which the spectral density of gamma transitions is proportional to the level density of the residual nucleus. Such an approach disregards the limitations imposed by the selection rules for the given type of transitions on the total number of possible transitions. Taking account of these rules for nuclei close to magic gives a considerably harder spectrum and higher cross-section of radiative capture occurring through the compound nucleus.

STRUCTURE OF THE SINGLE-PARTICLE SPECTRUM AND THE ENERGY DEPENDENCE OF σ_f/σ_n

A.V. Ignatyuk, G.N. Smirenkin and A.S. Tishin

The paper considers the drawbacks of the conventional method of analysing the energy dependence of σ_f/σ_n on the basis of the level density of the Fermi gas model. It is shown that the shell structure of the single-particle spectrum and the nucleon pairing effects substantially influence the trend of the fission and neutron widths, and that if these factors are taken into account it is possible to describe the observed behaviour of σ_f/σ_n both at high excitation energies and near the fission barrier.

LEVEL DENSITY AND STATISTICAL DESCRIPTION OF THE FISSION PROCESS

A.V. Ignatyuk

The paper reviews the models used at present to calculate the density of atomic nuclei excited states. Various experimental data which can be described by these models are considered.

DOUBLE DIFFERENTIAL CROSS-SECTIONS OF NEUTRON INELASTIC SCATTERING ON Fe AND Ni NUCLEI

G.Ya. Tertychnyj and Yu.N. Shubin

(submitted to "Yadernaya Fizika")

Until very recently particle spectra and their angular distributions at substantial excitation energies were analysed on the basis of a statistical approach without making sufficiently correct allowance for the contribution of each angular moment. In order to separate the contribution of the processes which occur without forming a compound nucleus, we need a more correct estimate of the fraction of the equilibrium process across the compound nucleus.

The double differential cross-sections for inelastic scattering of E_o = 14 MeV neutrons on ^{56}Fe and ^{58}Ni nuclei are here calculated on the basis of the Hauser-Feshbach statistical approach [1], taking account of the contribution of each angular moment, and the total neutron absorption cross-section and the spectrum integrated over the angles are also determined.

The calculation results indicate slight anisotropy in relation to angle 90°. Analysis showed that although the main contribution to the double differential inelastic scattering cross-section is made by the processes occurring across the compound nucleus, the contribution of the direct and pre-equilibrium mechanisms is also appreciable. Estimating the share of these processes in the form of the Griffin model [2] (25% on Fe and 20% on Ni) together with the calculated spectrum in the statistical model, it is possible to obtain values for the double differential cross-sections of the (n,2n) and (n,pn) reaction on ^{56}Fe and ^{58}Ni which agree with the experimental values to within acceptable limits of error.

REFERENCES

[1] HAUSER, W., FESHBACH, H., Phys. Rev. 87 2 (1952) 366.

[2] GRIFFIN, J.J., Phys. Rev. Lett. 17 (1966) 478.
BLANN, C.K., Nucl. Phys. A172 (1971) 225.

CALCULATION OF THE KINETIC ENERGIES OF FISSION FRAGMENTS IN THE LIQUID-DROP MODEL OF THE NUCLEUS

V.S. Stavinskij, I.R. Svin'in and A.A. Seregin

The kinetic energies of fission fragments are calculated on the basis of the liquid-drop model and making two assumptions:

1. Scission can also occur in deformations smaller than critical;
2. Scission occurs not only at the thinnest point of the neck. Two limiting cases are considered:
   (a) Fragments assuming an equilibrium form without changing the distance between their centres of gravity;
   (b) Fragments diverging without changing the form existing at the time of scission.

The results are compared with experimental data for the uranium-236 nucleus. The calculated region of possible kinetic energies in case (a) agrees satisfactorily with experiment.

SPIN DEPENDENCE OF THE DENSITY OF PARTICLE-HOLE STATES OF ATOMIC NUCLEI IN THE FERMI GAS MODEL

Yu.V. Sokolov

An expression is obtained in the Fermi gas model for the density of particle-hole states of atomic nuclei, with allowance for the total angular momentum I. The scatter of the distribution of states over I is studied.

NEUTRON SPECTRUM IN A HOMOGENEOUS MEDIUM CONTAINING ^{238}U AND H

A.P. Platonov and A.A. Luk'yanov

The paper describes the method and results of calculation of neutron collision density in an infinite homogeneous medium containing uranium-238 and hydrogen nuclei in the 1-500 eV energy region. It is shown that the density of collisions near individual scattering resonances differs substantially from the asymptotic density generally used in calculating resonance integrals and group characteristics.

EFFECTIVE HYDROGEN CONSTANTS FOR MULTIGROUP CALCULATIONS OF URANIUM-WATER REACTORS IN THE DIFFUSION-TRANSPORT APPROXIMATION

V.N. Gurin, A.M. Poplavko and K.E. Popova

Using the spectral programme [2], the authors have obtained 21-group effective hydrogen constants for calculating homogeneous uranium-water systems in the diffusion-transport approximation. The system of hydrogen constants given in the annex has been verified in calculations of K_{eff} and group fluxes for cylindrical and spherical reactors with and without a reflector. Analysis showed a satisfactory accuracy of the effective constants in the calculations of K_{eff} ($\pm$ 0.6%) and fluxes ($\pm$ 10%).

Nuclear Physics Institute of the Ukrainian SSR Academy of Sciences

TOTAL NEUTRON CROSS-SECTIONS OF ^{233}U AND ^{235}U AND THE SCATTERING CROSS-SECTION OF ^{233}U FOR SLOW NEUTRONS

V.P. Vertebnyj, M.F. Vlasov, V.V. Kolotyj,
M.V. Pasechnik, V.A. Pshenichnyj,
V.N. Urin and A.F. Fedorova

The total neutron cross-sections of ^{233}U were measured by the time-of-flight technique in the VVR-M reactor at the Nuclear Research Institute of the Ukrainian SSR Academy of Sciences. The measurements were carried out with two different spectrometers having different resolutions, and two sample thicknesses were used (see Table 1).

Table 1

Data on samples and measurement characteristics

Sample	Path length, m	Resolution, μsec/m	Sample thickness (nuclei/barn)	Neutron energy range
^{233}U		3	0.00998	$1 < E_n < 0.03$
^{233}U		6	0.0022	$0.2 < E_n < 0.01$
^{233}U	10.3	6	0.00998	$1 < E_n < 0.05$
^{235}U		6	0.0078	$1 < E_n < 0.01$
^{235}U		6	0.0024	$1 < E_n < 0.01$
^{233}U		1.7	0.0022	$1 < E_n < 0.03$
^{233}U	18.7	7	0.0022	$0.2 < E_n < 0.005$

The samples were in the form of disks 28 mm in diameter. Since the neutron beam had small width, the transmission was measured at different positions in order to eliminate local inhomogeneities in sample density. The samples were rotated about the axis parallel to the direction of the neutron beam.

Impurities did not contribute more than 0.1% of the value of the cross-section. In measurements with the sample in the beam, the minimum number of counts per channel was 20 000 and the maximum 100 000. The good agreement (within limits permitted by statistical fluctuations) of the measurements of total cross-sections in the region of overlap of different measurements indicates that there are no systematic errors in measurements with different spectrometers. The energy dependence of the total neutron cross-sections of ^{233}U, averaged over all measurements, is given in Table 2, which also shows the total measurement errors - the scatter of the results of different series of measurements.

The scattering cross-sections of ^{233}U were measured in 4π-geometry in relation to reference samples of vanadium and lead, the scattering cross-sections of which are taken as 5 and 11 barn respectively. The ^{233}U sample, 0.543 mm thick and 28 mm in diameter, was placed at the centre of an array of boron counters embracing the full solid angle for scattered neutrons. The neutron counting efficiency was of the order of 50% on average, the flight length being 5.1 m and resolution 25 μsec/m. To take account of the contribution of fast fission neutrons, the measurements were performed with and without a B_4C screen. Corrections were made for multiple scattering, and neutron attenuation in the sample after scattering was taken into account.

Table 3 gives the scattering cross-section values for energies > 0.1 eV, where the results are practically independent of the type of reference used and coherent effects are not significant.

The total neutron cross-section of uranium-235 was measured with a resolution of 6 μsec/m for two sample thicknesses (data are given in Table 1). The measurement conditions were similar to those for uranium-233. The energy dependence of the total neutron cross-sections of uranium-235 is contained in Table 4.

Table 2

Total neutron cross-sections of ^{233}U

Neutron energy E_n, eV	Total cross-section σ_t, barn	Neutron energy E_n, eV	Total cross-section σ_t, barn
0,939	I62 ± I	0,I65	25I ± 2
0,800	I48 ± 2	0,I38	265 ± 6
0,690	I45 ± 2	0,II3	288 ± 5
0,600	I52 ± 3	0,095	309 ± 4
0,528	I63 ± 2	0,085	330 ± 4
0,468	I70 ± 3	0,075	352 ± 5
0,4I7	I75 ± 2	0,0675	368 ± 6
0,375	I80 ± 7	0,0625	383 ± 3
0,338	I85 ± 5	0,0575	404 ± 5
0,307	I96 ± 2	0,0525	42I ± 5
0,279	204 ± 2	0,0475	442 ± 5
0,256	205 ± 2	0,0425	470 ± 3
0,235	220 ± 5	0,0375	499 ± 5
0,2I6	226 ± 3	0,0325	546 ± 8
0,I87	235 ± 2		

Table 3

Energy dependence of the scattering cross-section of uranium-233

Neutron energy E_n, eV	Scattering cross-section σ_t, barn	Neutron energy E_n, eV	Scattering cross-section σ_t, barn
0,46	I2,3 ± 0,3	0,I6	I3,I ± 0,3
0,37	I3,0 ± 0,3	0,I4	I3,0 ± 0,3
0,30	I3,3 ± 0,3	0,I2	I3,3 ± 0,3
0,25	I3,4 ± 0,3	0,II	I3,2 ± 0,3
0,2I	I3,2 ± 0,3	0,097	I3,2 ± 0,3
0,I8	I3,I ± 0,3		

Table 4

Energy dependence of the total neutron cross-section of uranium-235

Neutron energy E_n, eV	Total cross-section σ_t, barn	Neutron energy E_n, eV	Total cross-section σ_t, barn
0,939	87 ± 3	0,I62	244 ± 4
0,800	84 ± 3	0,I37	262 ± 5
0,690	84 ± 3	0,II2	297 ± 5
0,60I	93 ± 3	0,095	325 ± 5
0,528	I07 ± 3	0,085	349 ± 5
0,468	I24 ± 3	0,075	374 ± 5
0,4I7	I45 ± 3	0,0675	403 ± 5
0,375	I85 ± 4	0,0625	422 ± 5
0,338	222 ± 4	0,0575	43I ± 5
0,307	255 ± 4	0,0525	466 ± 5
0,279	250 ± 4	0,0475	494 ± 7
0,256	249 ± 4	0,0425	52I ± I0
0,235	239 ± 4		
0,2I6	233 ± 4		
0,I87	233 ± 4		

V.G. Khlopin Radium Institute of the USSR Academy of Sciences

SYMMETRICAL AND ASYMMETRICAL FISSION OF ^{226}Ra INDUCED BY 5-15 MeV NEUTRONS

E.A. Zhagrov, I.M. Kuks, Yu.A. Nemilov, Yu.A. Selitskij and V.B. Funshtejn

(Submitted to "Nuclear Physics")

The purpose of the work was to determine whether a symmetrical fission peak exists in the regions of excitation of nuclei before the beginning of emissive fission and find out how its value changes as a function of excitation energy. In the present work, the kinetic energy spectra of single fission fragments have been measured and the values of the cross-sections for fission of radium by neutrons have been refined.

A radium target weighing ~ 100 μg was fabricated from RaF_2 by vacuum evaporation. The fragment energy was measured with a silicon detector of the p-n type. The high specific alpha-activity of radium gives rise to considerable experimental difficulties associated with the radiation instability of the detector properties and the need for very high-speed electronic circuitry. Low-resistance silicon detectors (ϱ = 150 ohm.cm) were found to be the most suitable. A special electronic circuit was developed for discriminating the rare fragment pulses against the background of the higher repetition rate of pulses from alpha particles and their multiple random pile-up.

In all kinetic energy spectra for neutron-induced fission fragments of radium a pronounced minimum separates the peak of light asymmetric-fission fragments from the total distribution of heavy fragments and symmetric-fission fragments. This makes it possible to evaluate that fraction (denoted by s) of the total number of fissions which belongs to the central peak of the mass yield curve.

E_n(MeV)	5,0±0,2	6,4±0,2	7,8±0,4	9,5±0,3	I4,8
S	0,02±0,03	0,05±0,04	0,23±0,05	0,3I±0,03	0,62±0,04

The refined fission cross-section values are:

E_n(MeV)	5,8±0,I	6,3±0,I	6,6±0,3	7,3±0,3	7,9±0,5	8,7±0,5	9,5±0,3
σ_f(millibarn)	5,2±0,2	3,5±0,2	3,6±0,2	3,9±0,2	4,4±0,3	5,0±0,3	5,9±0,3

The most probable kinetic energies in the peaks of light and heavy symmetric-fission fragments are: E_ℓ = (100 ± 1) MeV, E_H = (63 ± 1) MeV, E_s = (77 ± 1) MeV. The most important results of the work are:

1. In the energy region near the fission barrier, radium undergoes asymmetric fission just as heavier nuclei;
2. At higher energies up to E_n = 9 MeV, where emissive fission does not occur, the fission of the ^{227}Ra compound nucleus is characterized by a three-hump mass yield curve.

REFERENCES

[1] JENSEN, R.C., FAIRHALL, A.W., Phys. Rev. 109 (1958) 942.

[2] BABENKO, Yu.A., NEMILOV, Yu.A., SELITSKIJ, Yu.A., FUNSHTEJN, V.B., Yad. Fiz. 7 (1968) 269.

BABENKO, Yu.A., IPPOLITOV, V.T., NEMILOV, Yu.A., SELITSKIJ, Yu.A., FUNSHTEJN, V.B., Yad. Fiz. 10 (1969) 233.

BABENKO, Yu.A., NEMILOV, Yu.A., PLESKACHEVSKIJ, L.A., SELITSKIJ, Yu.A., FUNSHTEJN, V.B., Yad. Fiz. 11 (1970) 1006.

[3] ZHAGROV, E.A., NEMILOV, Yu.A., SELITSKIJ, Yu.A., Yad. Fiz. 7 (1968) 264.

KINETIC ENERGY OF FISSION FRAGMENTS WITH EVEN AND ODD NUMBER OF PROTONS

S.M. Solov'ev and V.P. Ehjsmont

Because of pairing forces in fragments, the total instantaneous fission energy of an even-even nucleus in the case of division into fragments with even Z is approximately 2 MeV higher than in that with odd Z. In order to find out the mode of distribution of this excess energy, the authors carried out comparative measurements of the kinetic energies of fragments with even and odd charges. For this purpose, under double measurement conditions (in an AI-4096 analyser), the kinetic energy and X-ray spectra of fragments from ^{252}Cf spontaneous fission were determined with high statistical accuracy. Processing of the data (in a computer) did not show that any noticeable fraction of the excess energy was associated with the kinetic energy of fragments.

FISSION X-RAY SPECTRA FOR DIFFERENT KINETIC ENERGIES OF A LIGHT FRAGMENT AND THE "FINE" STRUCTURE OF MASS YIELD

A.G. Donichkin, S.M. Solov'ev and V.P. Ehjsmont

For the case of ^{252}Cf spontaneous fission, the spectra of the K-series of characteristic radiation of heavy fragments were measured at different light-fragment kinetic energies. The energies of X-ray quanta and of fragments were measured by means of diffusion-drift and surface-barrier semiconductor detectors respectively. Components corresponding to specific charges (elements) were separated in the spectra by the method of least squares in a Minsk-22 computer. Assuming that the relative yields of these components characterize the charge yields, it is concluded that there is a predominant probability for the formation of fragments with an even number of protons at high kinetic energies - low excitation energies of fragments. It is this which provides experimental justification for the existing hypothesis that "fine" structure is by nature a structure deriving from the energy efficiency of even-even nucleus formation.

THE TIME OF X-RAY EMISSION BY FIXED-CHARGE FRAGMENTS

A.G. Donichkin, S.M. Solov'ev and V.P. Ehjsmont

The authors have measured the energy distributions of the K-series of characteristic rays emitted by fragments at rest and in motion relative to the radiation detector. The measurements were carried out with the help of semiconductor detectors of electromagnetic radiation and fission fragments. Components corresponding to the individual elements were separated in the experimental distributions by the method of least squares in a computer. From changes in intensity of these components as a function of the state of motion, lifetimes with respect to X-ray emission were determined in the case of heavy fragments of fixed charge. These times vary within the range 0.2-1.2 nsec for Z = 53-61. Fragments with charge 54 and 56 have shorter half-lives than the neighbouring nuclei with odd Z. This is associated with the level structure of even-even nuclei near closed shells.

All-Union Scientific Research Institute of Physical and Radio Engineering

EXTRAPOLATION METHOD OF DETERMINING THE SPECTRAL COEFFICIENT OF THE REACTOR NEUTRON FIELD

R.D. Vasil'ev, E.I. Grigor'ev, G.B. Tarnovskij and V.P. Yaryna

The paper describes a method of determining the spectral coefficient $g_{o,1} = \Phi_{o,1}/\Phi_s$, where $\Phi_{o,1}$ and Φ_s are the integral density of the flux of <0.1 MeV neutrons and of the effective energy threshold of the $^{32}S(n,p)^{32}P$ reaction, respectively. The procedure has been developed for application to the activation method of measuring the in-reactor fast neutron spectrum.

The extrapolation method comprises measurement of the integral neutron flux density values for several energy values above 0.5 MeV, determination of the function approximating the integral spectrum from the measurement results, and valid extrapolation of the dependence obtained to 0.1 MeV.

The authors give the recommended form of the function approximating the integral spectrum in the 0.1-3 MeV energy region. The problem of the errors of determining the spectral coefficient is considered. Values are given for the coefficient $g_{o,1}$ of the neutron field of a fast reactor.

CALIBRATION OF RHODIUM ACTIVATION KIT

R.D. Vasil'ev, E.I. Grigor'ev and V.P. Yaryna

The authors describe the rhodium neutron-activation kit designed for measuring neutron field characteristics, and the procedure for calibrating it. The kit includes rhodium detectors used for neutron counting in accordance with the $^{105}Rh(n,n')^{103m}Rh$ reaction and a ^{241}Am calibration source with previously determined activity, in relation to which the induced activity of the rhodium detectors is determined with application of appropriate correction factors.

The activity of the calibration source is measured in relation to the known activity of one of the rhodium detectors pre-irradiated in a reference field of 14 MeV neutrons. The radiation characteristics of the reference field were determined in advance. The field was created with a neutron generator giving stable radiation characteristics to within $\pm$ 0.5%.

The ^{241}Am calibration source can be used to measure the induced activity of rhodium detectors to within 5-7%.

I.V. Kurchatov Institute of Atomic Energy

PENETRATION OF THE TWO-HUMP POTENTIAL BARRIER

A.S. Tyapin and V.E. Marshalkin

It has been found that the penetration and reflection factors of two-hump barriers with a well-developed well between the humps are:

$$P = \frac{P_A \cdot P_B}{\exp(\eta) + T_A \cdot T_B \cdot \exp(-\eta) + 2\sqrt{T_A \cdot T_B} \cdot \cos\theta}, \quad (1)$$

$$T = \frac{T_A \cdot \exp(\eta) + T_B \cdot \exp(-\eta) + 2\sqrt{T_A \cdot T_B} \cdot \cos\theta}{\exp(\eta) + T_A \cdot T_B \cdot \exp(-\eta) + 2\sqrt{T_A \cdot T_B} \cdot \cos\theta}, \quad (2)$$

where $P_{A,B}$ is penetration of barriers A and B respectively, and $T_{A,B} = 1 - P_{A,B}$. ϑ and η are the real and imaginary parts of phase φ. To calculate phase φ, it is necessary to apply a quasi-classical approximation and replace the expression obtained by an expression which is analytical for $\lambda_{A,B} \to 0$, the quasi-classical phase being the asymptotic form of the latter expression for large λ. Here $\lambda_{A,B} = \frac{-E + V_{A,B}}{\hbar\omega_{A,B}}$, where E is incident particle energy, and $V_{A,B}$ and $\hbar\omega_{A,B}$ are respectively the heights and frequencies of barriers A and B. In the deep sub-barrier region, expression (1) coincides with the corresponding expression in Ref. [1] and, in addition, is valid in the near-threshold region. In the case of a barrier in the form of two inverted parabolas with break at z = 0

$$\theta = \sum_{\kappa=A,B} \left\{ y_\kappa \sqrt{y_\kappa^2 - 2\lambda_\kappa} - 2\lambda_\kappa \left[\ln\left(y_\kappa + \sqrt{y_\kappa^2 - 2\lambda_\kappa}\right) - \right.\right.$$
$$\left.\left. - \frac{1}{2} - \frac{1}{2}\ln 2 \right] - \arg\Gamma\left(\frac{1}{2} - i\lambda_\kappa\right) \right\}, \quad (3)$$

where $\arg\Gamma(x)$ is the argument of the gamma function, $y_{A,B} = \sqrt{\frac{m\omega_{A,B}}{\hbar}}\, z_{A,B}$; m is the incident particle mass, and $z_{A,B}$ is the position of the maxima of humps A and B. To evaluate the influence of the imaginary term in the fission potential, it is evidently sufficient to consider that dissipative processes shift the position of the resonance points in the complex plane of variable E upwards

along the imaginary axis by a small amount iw_o. In the deep sub-barrier region this means that the imaginary term in the fission potential is small, negative and constant in the quasi-classically allowed region between the humps. In this case $\eta = w_o \cdot \frac{d\vartheta}{dE}$.

The penetrations of two-hump fission barriers calculated by this method are shown in Figs 1-3. It will be seen from these figures that there is a resonance structure on the penetration curve near the threshold, but it is much less pronounced than in the deep sub-threshold region. The imaginary part of the fission potential influences the penetration curve near the threshold in a substantially different manner from what it does deep under the barrier. Penetration of barriers with a non-zero imaginary part is close to unity only at very high energies.

REFERENCES

[1] GAJ, E.V., IGNATYUK, A.V., RABOTNOV, N.S., SMIRENKIN, G.N., Yad. Fiz. 10 (1969) 542.

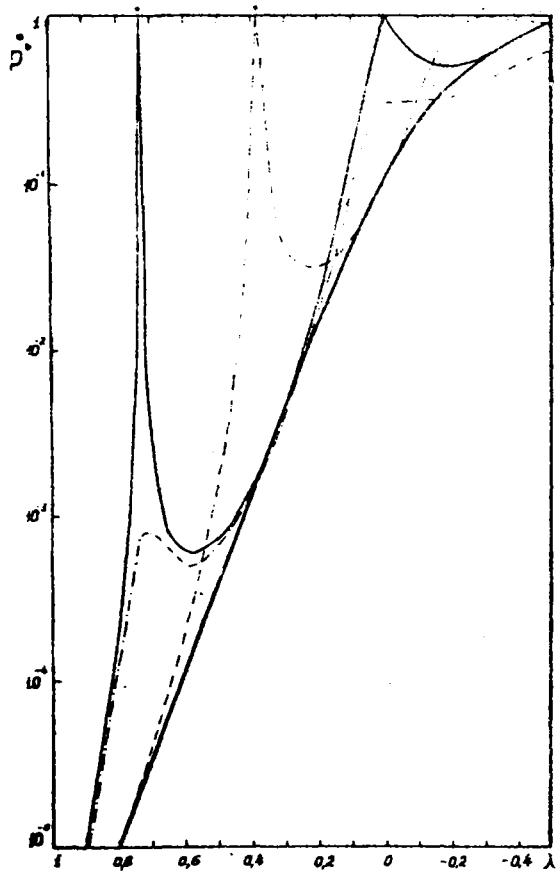

Fig. 1 Penetration of symmetrical two-hump barrier. The continuous resonance curve represents the position of the resonance at the barrier peak, and the dashed curve the resonance raised by $0.3\,\hbar\omega$ above the barrier, the smooth continuous curve being P_{min}. The dot-dash curve corresponds to the presence of imaginary potential in the classically allowed region between the humps.

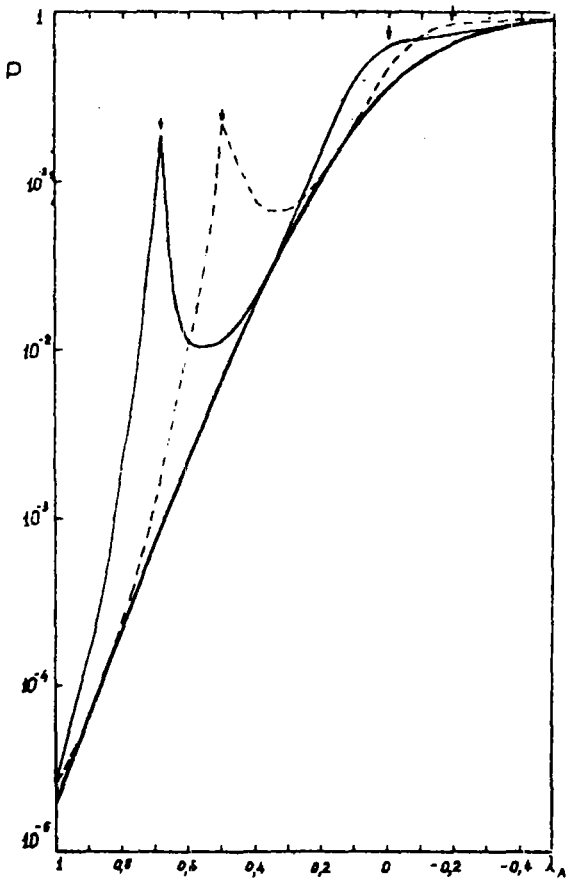

Fig. 2 Penetration of the two-hump barrier. $\hbar\omega_A = \hbar\omega_B = \hbar\omega$, $V_A - V_B = 0.5\hbar\omega$. The remaining notations are the same as in Fig. 1.

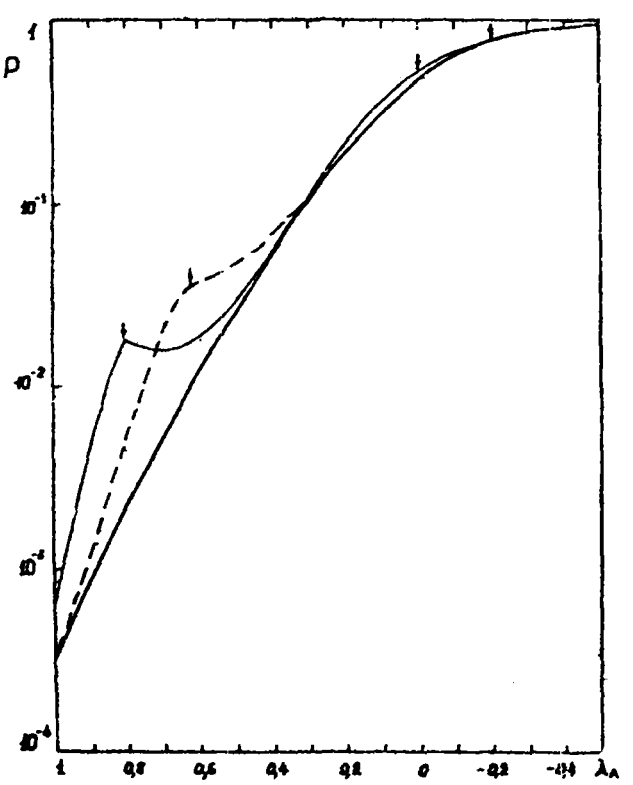

Fig. 3 Penetration of the two-hump barrier. $\hbar\omega_A = \hbar\omega_B = \hbar\omega$, $V_A - V_B = 1\hbar\omega$. The remaining notations are the same as in Fig. 1.

VARIATION OF FISSION-FRAGMENT MASS DISTRIBUTION WITH NEUTRON ENERGY

S.M. Dubrovina, V.I. Novgorodtseva, L.N. Morozov, V.A. Pchelin, L.V. Chistyakov, V.A. Shigin and V.M. Shubko

The paper presents the radiochemical measurements of the yields of a number of neutron-induced fission fragments of ^{232}Th. The measurements were carried out in the 1.5-18 MeV neutron energy range. In that range the yield of symmetrical fission (^{115}Cd) increases from 1/50 000 to 1/7 and that of "strongly asymmetrical" fission (^{77}As) from 1/1700 to 1/110 in relation to the yield of the most probable asymmetrical fission (^{89}Sr). The yields of various fragments in relation to ^{89}Sr yield are given in Table 1 below. The measurement accuracy ≈ 10% except in the case of very small yields, where it is ≈ 20%. Neutron energy ΔE_n and energy re resolution are expressed in MeV.

Table 1

E_n	ΔE_n	As^{77}	Se^{89}	Mo^{99}	Cd^{115}	Sn^{121}	Sn^{125}	Sb^{127}	Ba^{140}
I,53	0,I	-	I,0	0,37	$\leq 3{,}2.10^{-5}$	$\leq 9.10^{-4}$	-	-	I,2
I,65	0,I	$\leq 0.10^{-4}$	I,0	0,36	$\leq 1{,}9.10^{-5}$	-	$8{,}9.10^{-5}$	$6{,}3.10^{-4}$	I,I
2,0	0,I	-	I,0	0,36	$2{,}2.10^{-4}$	$3{,}3.10^{-4}$	$3{,}9.10^{-4}$	-	-
3,0	0,I5	$I{,}8.10^{-3}$	I,0	0,37	$2{,}3.10^{-3}$	$I{,}6.10^{-3}$	$6{,}7.10^{-4}$	-	I,I
3,9	0,I5	$4{,}0.10^{-3}$	I,0	0,34	$6{,}I.10^{-3}$	$5{,}9.10^{-3}$	$I{,}4.10^{-4}$	-	I,2
4,8	0,I	$5{,}I.10^{-3}$	I,0	-	$I{,}6.10^{-2}$	-	$4{,}7.10^{-3}$	-	-
I3	0,I5	$7{,}5.10^{-3}$	I,0	0,35	$I{,}6.10^{-I}$	$I{,}2.10^{-I}$	5.10^{-2}	-	I,2
I5	0,25	7.10^{-3}	I,0	0,36	$I{,}6.10^{-I}$	$I{,}0.10^{-I}$	$4{,}7.10^{-2}$	-	0,9
I7,7	0,I5	9.10^{-3}	I,0	0,37	$I{,}4.10^{-I}$	$I{,}I.10^{-I}$	$4{,}9.10^{-2}$	$2{,}2.10^{-2}$	I,0